Simulation and Analysis of an Alkaline Electrolysis System for Hydrogen Production using ASPEN Plus Model

Anand Kumar Pandey*, Nihal Patel*, and Amarjeet Singh**

Abstract - A semi-empirical mathematical model is presented in this work to predict the electro-chemical behaviour of an alkaline water electrolysis system. It is based on the polarisation curve and Faraday performance characteristics and takes into account factors such as temperature, pressure variations, and current density. Low hydrogen impurity levels and small voltage variations are shown by evaluation, showing good agreement with real data. The model helps with the design and optimisation of electrolyzers, and sensitivity analysis helps discover important operational aspects. It also suggests a thorough model that combines plant and stack stability that was created with Aspen Custom Modeller without the need for coding expertise. The study suggests a temperature rise and a pressure drop for improved system capacity, with an emphasis on using parametric research and simulations to maximise hydrogen generation efficiency and plant stability.

Keywords: ASPEN Plus, electrochemical, electrolyzer, efficiency, over-potential.

1. INTRODUCTION

A key instrument in this effort is hydrogen, which has the ability to decarbonise difficult-to-abate industries and function as a low-carbon energy source [1]. Although the idea of a "hydrogen economy" has been around for more than 20 years, high manufacturing costs and a sluggish corporate response to climate concerns have made it less viable [2,3]. However, new developments in technology and a change in the mindset of the fossil fuel business have reignited interest in hydrogen as an essential component of the global drive towards decarbonisation.

Numerous energy analysts predict a large rise in hydrogen production, despite divergent predictions for hydrogen consumption and disagreements over its applicability for different uses, such as heating and heavy transportation [5]. It is imperative, therefore, to conduct a thorough assessment of the environmental effects of hydrogen generation and use, taking into account variables other than carbon emissions [6]. While comparing various hydrogen generation paths has been the main focus of life cycle analysis research, these studies frequently lack a worldwide contextualization to ascertain their absolute sustainability [7].

When estimating the potential environmental effects of hydrogen technologies, prospective life cycle assessments (pLCAs) are proving to be an effective tool [8,9]. This is because they take into account advancements in technology as well as the larger picture of global decarbonisation initiatives [10]. In these evaluations, harmonising methods and system limits can offer greater insights into how sustainable various hydrogen generation paths are in comparison [11,12]. In general, t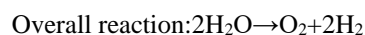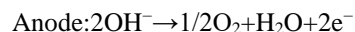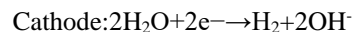hese evaluations are necessary to make well-informed judgements on hydrogen's place in a future energy system that is sustainable [13-15].

There are four basic approach for producing Hydrogen using electrolysis principle and, the methods are Simple Alkaline electrolysis, Anion exchange membrane (AEM), Proton exchange membrane (PEM) & High temperature electrolysis also known as Solid Oxide electrolysis [16,17]. In this paper we use simple alkaline electrolysis for the production of hydrogen.

In this paper we use ASPEN PLUS software for analyzing various parameters which affects the electrolysis process. These parameters are over-potential, effect of temperature, effect of pressure, stack power, current density and heat produced in the electrolytic chamber. We use 35% w/v KOH for making the solution alkaline. We Start our simulation at 40°C and extend our simulation up to 80°C. We will vary the pressure from 2 bar to 10 bar and calculate various parameters. We use ASPEN plus software for this simulation because this Software does not require any coding skill for process simulation. This paper also consists of various plots of efficiencies of the stack with different power inputs.

2. ALKALINE ELECTROLYSIS

Alkaline electrolysis is a method of production of hydrogen and oxygen by breaking water molecules in the alkaline solution. The charge carrier in alkaline electrolysis is OH^- Following reaction occur in alkaline electrolysis:

$$Cathode: 2H_2O + 2e^- \rightarrow H_2 + 2OH^-$$

$$Anode: 2OH^- \rightarrow 1/2 O_2 + H_2O + 2e^-$$

$$Overall\ reaction: 2H_2O \rightarrow O_2 + 2H_2$$

---

*Department of Electrical and Electronics Engineering, JSS Academy of Technical Education, Noida, India.
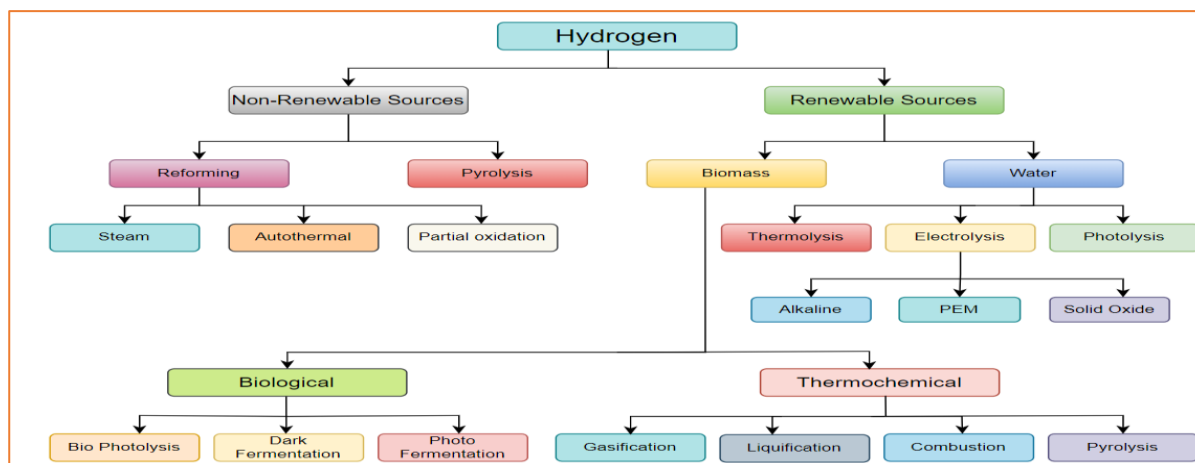
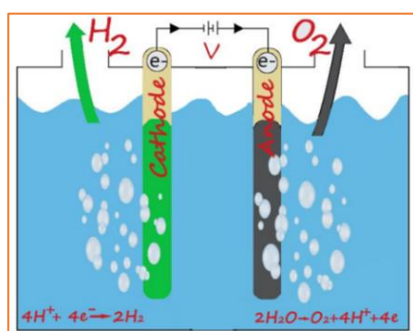**Fig 1.1. Different methods of production of hydrogen.**

Fig 1.2. Electrolytic chamber for alkaline electrolysis.

By varying the current density, the main goal of this work is to thoroughly understand the properties of alkaline electrolyzers [17]. The knowledge gleaned from this work is meant to aid in the creation of an extremely effective PV-electrolysis-linked system [18]. The study examines the connection between alkaline electrolyzer performance and electrode size [19]. The experiment uses electrodes that consistently have a catalyst loading of 2 mg/cm^2 and keeps current densities between 0.2 and 0.3 A/cm^2, [20] which is a range that is shared by all the catalysts employed. Intriguing tendencies are revealed in the generated data. Up to a threshold size, the amount of hydrogen created initially grows proportionally with electrode size. Around 4.5 cm^2 represents the electrode size at which hydrogen generation reaches this crucial threshold [21].

Considering these findings, the paper admits that increased current densities result in higher voltage needs for the electrolyzer. Electrolyzer resistance and a kinetic parameter, K, are included in a model that is presented to quantify this voltage rise [22, 23]. The study's conclusion emphasizes the significance of choosing the best operating points for the PV-electrolysis coupled system while considering variables like hydrogen production, solar irradiance, and investment costs. By using a comprehensive approach, it is ensured that the proposed system would support efficient and sustainable hydrogen generation.

As the current density increases, so do the voltage requirements for the electrolyzer. This relationship was modelled with different electrolyzer resistances and a kinetic component known as "K." To get the optimum overall conversion efficiency, the operating point must minimise investment costs for the concentrated PV-electrolysis system while optimising hydrogen output given solar irradiance. In general, when power is generated from electrochemical sources, the electrode operating potential is represented by the symbol "Vop," while the electrochemical power source's equilibrium potential is represented by the symbol "E." The following relations can be used to compute the power [24, 25].

$$P \propto (V_{op} - E_o)^2$$

The practical potential of Electrode is slightly less than V_{op} due to voltage drop caused by the resistance of the cell so eq(1) can be written as.

$$P = K(V_{op} - I.R - E_o)^2$$

The ability of the electrolyzer to convert electrical energy into chemical energy is represented by the coefficient "K," which acts as the proportionality factor in power conversion.

3. METHODOLOGY

In this project we use ASPEN Plus simulation software for our simulation. The simulation model is shown in

Figure 1.3. In this model we use 35% w/v KOH for making the solution alkaline. We Start our simulation at 40°C and extend our simulation up to 80°C. We will vary the pressure from 2 bar to 10 bar and calculate various parameters. Since both oxygen and hydrogen are produced in the same chamber, we need a Separator for separating Oxygen and Hydrogen. We place two separator blocks for the separation of Oxygen and Hydrogen [26]. We use two water traps for separating water vapour mix with the gases. For calculating polarization curve we use the formula mentioned below.

$$V_{cell}=V_{rev} +[(r_1+d_1)+r_2.T+d_2.p]I+s.\log[(t_1+t_2/T+t_3/T^2)i+1]$$

The values parameters used in the formula is given in the following table.

**Table 1.1 Constants used in calculating various parameters of the electrolytic chamber.**

Terms	Value	Unit
V_0	1.23	V
s	0.3382400	V
t_1	-0.0153900	m^2/A
t_2	2.0018100	$m^2 °C/A$
t_3	15.2417800	$m^2 °C^2/A$
f_{11}	478645.74	A^2/m^4
f_{12}	-2953.15	$A^2/m^4 °C$
LHV H_2	33.33	kWh/kg
ΔG	237.13	kJ
r_1	0.0000445	$\Omega\ m^2$
r_2	0.0000000	$\Omega\ m^2/ °C$
d_1	-0.0000031	$\Omega\ m^2$
d_2	0.0000004	$\Omega\ m^2/bar$
Faraday constant	96485	C/mol
f_{21}	1.0396000	
f_{22}	-0.00104	$°C^{-1}$
Delta S	0.163422	kJ/K
ΔH	293.1837460	kJ

This model of an alkaline water electrolysis system was made using Aspen Plus and includes the alkaline electrolysis cell stack and plant balancing. Hydrogen and oxygen are produced from water via an electrochemical process in the cell stack, the main component of the system. Recirculation pumps bring the electrolyte back to the stack after it has been separated from the gas in the liquid-gas separation vessels containing the hydrogen and oxygen that have been produced. With the help of heat exchangers included into the electrolyte recirculation loops, the cooling circuit's cooling pump and air cooler circulate cooling water to remove waste heat and maintain a constant temperature inside the cells.

Aspen Custom Modeller was used to develop a custom operation unit that would contain the alkaline water electrolysis stack model for system simulation in Aspen Plus. Included in the produced stack operating unit are the electrochemical model for the alkaline electrolysis cells as well as all the equations related to the mass and energy balances that occur in the stack. One may use the ACM tool to make a bespoke icon that links many job, material, or heat streams. Following simulation, the model is added to the standard operational unit palette and exported to the Aspen Plus Library.

For alkaline electrolysis cells, an electrochemical model has also been created that forecasts a stack's electrochemical behaviour under various operating circumstances, including pressure and temperature. The model is able to determine the polarisation curve, Faraday efficiency, and gas purity as a function of current by using statistical data and scientific principles. The cell voltage is always greater than the theoretical reversible voltage due to overpotentials caused by kinetic and resistive forces.
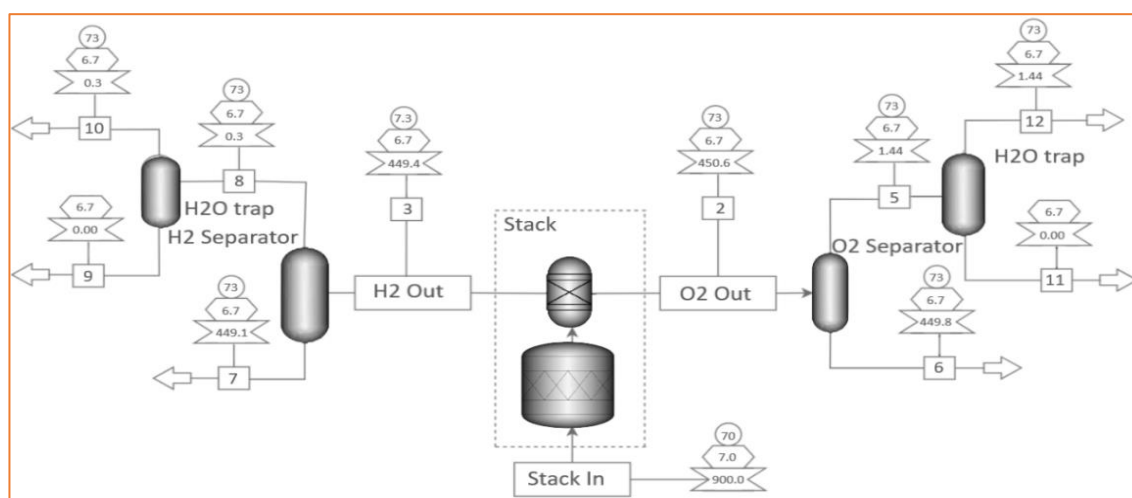
Fig 1.3 ASPEN Plus model of alkaline electrolysis.

All the machinery required to run the stack, such as the cooling loop, circulation pumps, heat exchangers, gas-liquid separator vessels, and deionized water supply, is included in the balance of plant. The process

flow model has been created to incorporate each of the main elements found in a real alkaline electrolysis plant.

Most of the plant's balancing components have been replicated with standard components of Aspen Plus software. The Aspen software predicts fluid conditions surrounding the system, including thermodynamic data for all chemical species involved in the process, in addition to performing energy and mass balances across all components and adding system boundary conditions, individual component efficiencies, and operating parameters to the process.

4.   RESULT AND DISCUSSION

The breakdown of water is started at a voltage of 1.23V but due to extra resistance offered by the electrode, electrolytic solution and the gaseous molecules formed in the electrolysis an extra voltage is required for this. This extra voltage is known as overvoltage or overpotential as shown in Table 1.2. The graph mentioned in Figure 1.4 is the curve plotted between overvoltage and current density of an electrolytic chamber at a temperature of 60°C. In this curve we see that the overpotential increases with increase in current density. As current density increases the number of charges in the electrolytic chamber is also increased which increased the collision of the gaseous molecules and extra overpotential is required to start the electrolysis reaction. When the temperature of the electrolytic chamber is increased the overpotential decreases as shown in Table 1.3 and Figure 1.5.

Table 1.2. Cell voltage V/s current density at different pressures at constant temp of 60°C.

Current Density	V (2 bar)	V (4 bar)	V (6 bar)	V (8 bar)	V (10 bar)
1000	1.7346	1.7354	1.7264	1.7372	1.7381
2000	1.8759	1.8777	1.8794	1.8812	1.8830
3000	1.9770	1.9797	1.9824	1.9851	1.9878
4000	2.0614	2.0650	2.0686	2.0722	2.0758
5000	2.1366	2.1411	2.1455	2.1500	2.1545
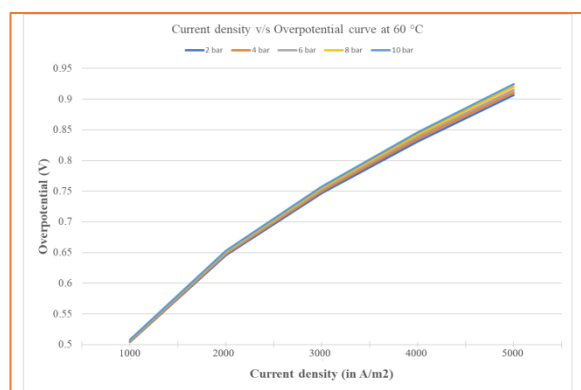
Fig. 1.4. Plot between over-potential and the current density of electrode of alkaline electrolysis at 60°C.

Table 1.3. Cell voltage V/s current density at different pressures at constant temp of 80°C.

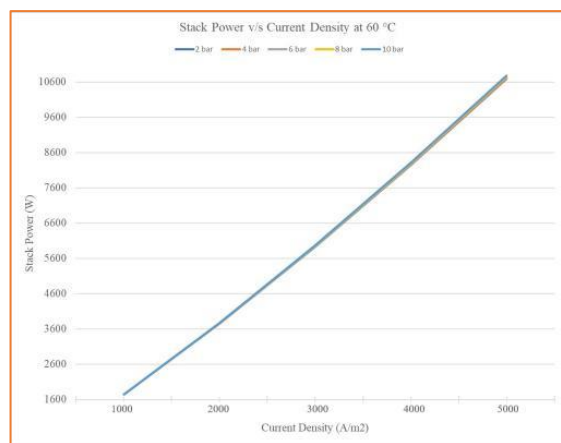| Current Density	V (2 bar)	V (4 bar)	V (6 bar)	V (8 bar)	V (10 bar)
1000	1.6497	1.6506	1.6515	1.6524	1.6533
2000	1.7886	1.7904	1.7922	1.7940	1.7958
3000	1.8890	1.8917	1.8945	1.8971	1.8998
4000	1.9731	1.9767	1.9803	1.9839	1.9874
5000	2.0481	2.0526	2.0571	2.0616	2.0660
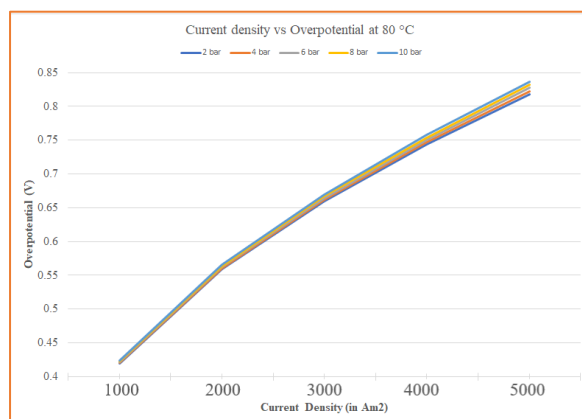
Fig. 1.5. Plot between over-potential and the current density of electrode of alkaline electrolysis at 80°C.

The stack power is the power supplied to the electrolytic chamber to start the electrolytic reaction. The fig 1.6 given below is the plot between stack power and the current density at 60°C. In this plot when the current density increases the stack power is also increased because when the current density is high, high amount of current is required to flow through the electrode and power is directly proportional to the current, so power is automatically increases. All the pressure curve is almost colinear, so we can say that the stack power is independent of pressure. The fig 1.7 given below is the plot between stack power and the current density at 80°C. The stack power is reduced by a very little amount, so we conclude that the stack power is independent of temperature.

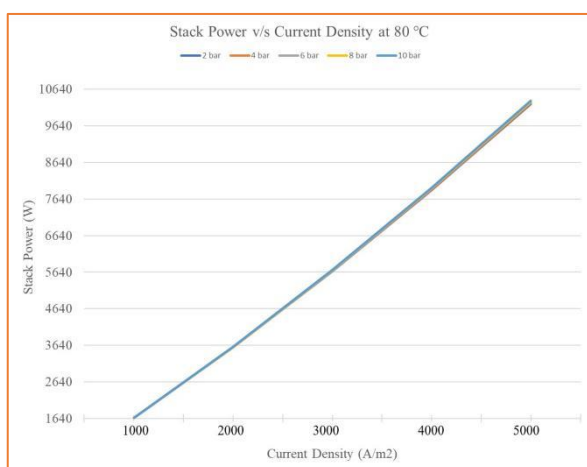**Table 1.4. Stack power V/s current density at different pressures at constant temp of 60°C.**

Current Density	V (2 bar)	V (4 bar)	V (6 bar)	V (8 bar)	V (10 bar)
1000	1734.6	1735.4	1736.3	1737.2	1738.17
2000	3751.8	3755.4	3758.9	3762.5	3766.14
3000	5931.2	5939.3	5947.3	5955.4	5963.45
4000	8245.9	8260.2	8274.6	8288.9	8303.21
5000	10683	10705	10727.9	10750	10772.6

Fig. 1.6. Plot between stack power and current density at a temperature of 60°C at different pressures.

Table 1.5. Stack power V/s current density at different pressures at constant temp of 80°C.

| Current Density	V (2 bar)	V (4 bar)	V (6 bar)	V (8 bar)	V (10 bar)
1000	1649.7	1650.6	1651.5	1652.4	1653.3
2000	3577.3	3580.9	3584.4	3588.1	3591.6
3000	5667.2	5675.3	5683.3	5691.4	5699.4
4000	7892.7	7907.0	7921.3	7935.6	7949.9
5000	10240	10263	10285	10308.0	10330.4

Fig. 1.7. Plot between stack power and current density at a temperature of 80°C at different pressures.

In the given Figure 1.8 the plot between hydrogen flow with respect to the current density at different temperatures. The hydrogen production is totally dependent on the charges flow through the electrolytic solution. As charge density increases the charge is also increased so the production of hydrogen is also increased so the flow rate of hydrogen is also increases. After a great increase in current density the hydrogen flow rate is decreased because of extra collision of the molecules of the gases produced in the electrolytic reaction.
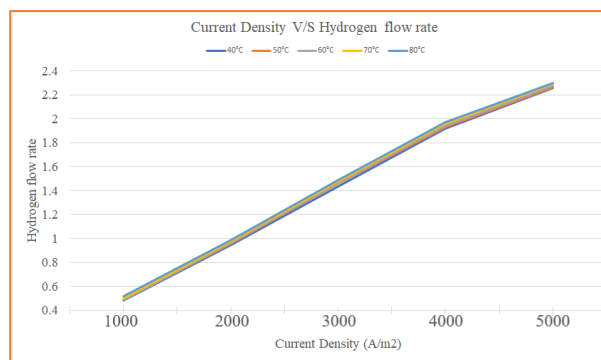
**Fig. 1.8. Plot between hydrogen flow rate and current density at different temperatures.**

The plot of the Faraday efficiency against the current density at various temperatures is shown in Figure 1.9. The Faraday efficiency increases quickly and saturates at a particular current density, as is evident. Low current density results in higher faraday efficiency at low temperatures, but high current density has the opposite effect as temperatures rise.
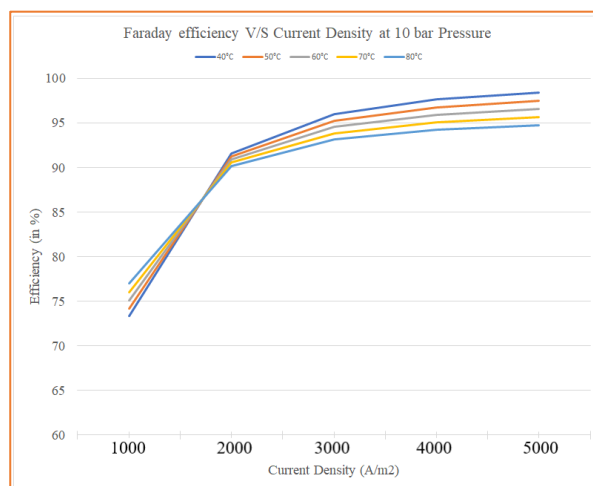

Fig. 1.9. Plot between Faraday efficiency and current density at different temperatures.

Figure 1.10 shows the variation between the production of heat in the electrolytic chamber with current density at different temperatures. The heat produced is dependent on the current and the thermo-neutral voltage. As current density increases the heat is also increased and the thermoneutral voltage is decrease with increase with temperature, but the decrement is very little as compared to the increment due to increment with increment in current density, so the overall heat production is increased with increase in current density.
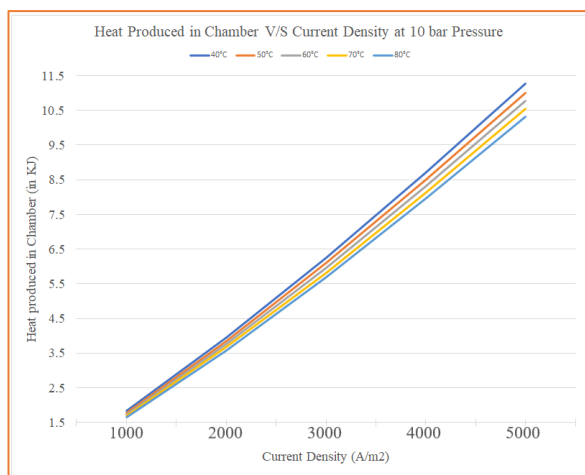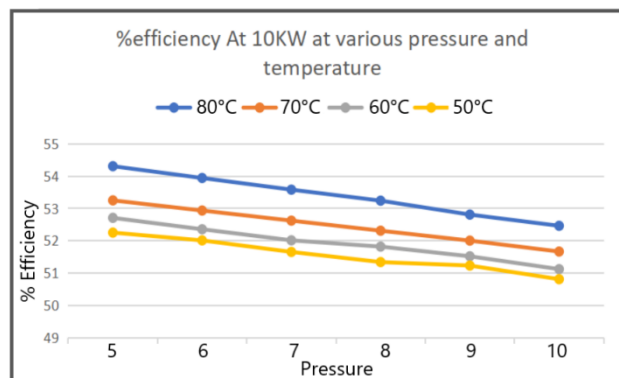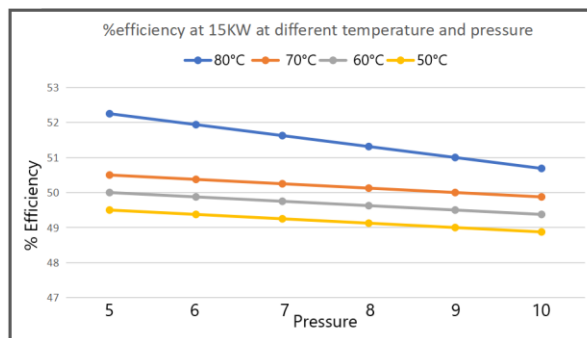
Fig. 1.10. Variation between the production of heat in the electrolytic chamber with current density at different temperatures.
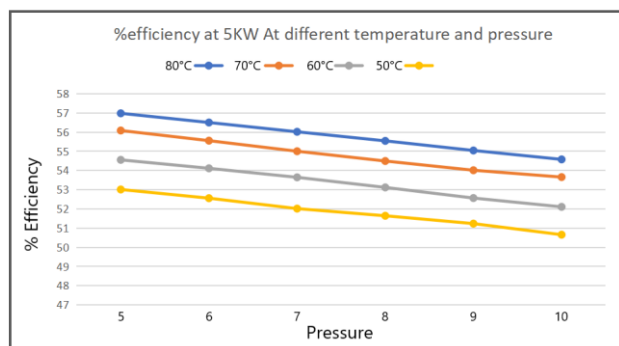
Fig. 1.11. Stack efficiency at 5kW for different temperatures and pressure.

Fig. 1.12. Stack efficiency at 10kW for different temperatures and pressure.

Fig. 1.13. Stack efficiency at 15kW for different temperatures and pressure.

5. CONCLUSION

The Aspen Plus model for an alkaline water electrolysis plant is suggested in the study in order to assess the system's performance in various operating scenarios. Standard operating units are used for the other components in the model, and Aspen Custom Modeller is used to incorporate a custom model of the electrolysis cells as a subroutine.

An excellent correlation between predicted values and experimental data was used to confirm the correctness of the model. Parametric research demonstrating that a temperature increase causes a decrease in the hydrogen rate because of a decrease in Faraday efficiency and an increase in the crossover of hydrogen to the oxygen side. As pressure rises, so does the stack voltage and the number of impurities in the gases that are created.

This research introduces a new Aspen Plus model that allows behaviour study of alkaline electrolyte systems to generate hydrogen using renewable energy sources. The model makes it possible to identify significant changes that may be optimised, resulting in a system with increased overall usefulness and efficiency. The findings indicate that operating temperature has a bigger impact than pressure, and that 5 bar and 80C are the ideal operating parameters for this system, which would produce an efficiency that is over 58% overall.

REFERENCES

[1] Andriani, Dindha, and Yusuf Bicer. "A review of hydrogen production from onboard ammonia decomposition: Maritime applications of concentrated solar energy and boil-off gas recovery." Fuel 352 (2023): 128900.

[2] Wang, Gang, Yuechao Chao, Tieliu Jiang, Jianqing Lin, Haichao Peng, Hongtao Chen, and Zeshao Chen. "Analyzing the effects of government policy and solar photovoltaic hydrogen production on promoting CO2 capture and utilization by using evolutionary game analysis." Energy Strategy Reviews 45 (2023): 101044.

[3] Tleubergenova, Akmaral, Yerdaulet Abuov, Saniya Danenova, Nurgabyl Khoyashov, Amina

Togay, and Woojin Lee. "Resource assessment for green hydrogen production in Kazakhstan." International Journal of Hydrogen Energy 48, no. 43 (2023): 16232-16245.

[4] Wang, Changlong, Stuart DC Walsh, Zhehan Weng, Marcus W. Haynes, Daisy Summerfield, and Andrew Feitz. "Green steel: Synergies between the Australian iron ore industry and the production of green hydrogen." International Journal of Hydrogen Energy 48, no. 83 (2023): 32277-32293.

[5] Moradpoor, Iraj, Sanna Syri, and Annukka Santasalo-Aarnio. "Green hydrogen production for oil refining–Finnish case." Renewable and Sustainable Energy Reviews 175 (2023): 113159.

[6] Al-Orabi, Ahmed M., Mohamed G. Osman, and Bishoy E. Sedhom. "Evaluation of green hydrogen production using solar, wind, and hybrid technologies under various technical and financial scenarios for multi-sites in Egypt." International Journal of Hydrogen Energy 48, no. 98 (2023): 38535-38556.

[7] Hassan, Qusay, Majid K. Abbas, Vahid Sohrabi Tabar, Sajjad Tohidi, Marek Jaszczur, Imad Saeed Abdulrahman, and Hayder M. Salman. "Modelling and analysis of green hydrogen production by solar energy." Energy Harvesting and Systems 10, no. 2 (2023): 229-245.

[8] Hassan, Qusay, Vahid Sohrabi Tabar, Aws Zuhair Sameen, Hayder M. Salman, and Marek Jaszczur. "A review of green hydrogen production based on solar energy; techniques and methods." Energy Harvesting and Systems 11, no. 1 (2024): 20220134.

[9] Hassan, Qusay, Aws Zuhair Sameen, Hayder M. Salman, and Marek Jaszczur. "Large-scale green hydrogen production using alkaline water electrolysis based on seasonal solar radiation." Energy Harvesting and Systems 11, no. 1 (2024): 20230011.

[10] Syed, Miswar Akhtar, and Muhammad Khalid. "An intelligent model predictive control strategy for stable solar-wind renewable power dispatch coupled with hydrogen electrolyzer and battery energy storage." International Journal of Energy Research 2023 (2023).

[11] Song, Shaojie, Haiyang Lin, Peter Sherman, Xi Yang, Shi Chen, Xi Lu, Tianguang Lu, Xinyu Chen, and Michael B. McElroy. "Deep decarbonization of the Indian economy: 2050 prospects for wind, solar, and green hydrogen." Iscience 25, no. 6 (2022).

[12] Schmitt, Erica A., Margot Guidat, Max Nusshör, Anna-Lena Renz, Kristof Möller, Marco Flieg, Daniel Lörch, Moritz Kölbach, and Matthias M. May. "Photoelectrochemical Schlenk cell functionalization of multi-junction water-splitting photoelectrodes." Cell Reports Physical Science 4, no. 10 (2023).

[13] Terlouw, Tom, Christian Bauer, Russell McKenna, and Marco Mazzotti. "Large-scale hydrogen production via water electrolysis: a techno-economic and environmental assessment." Energy & Environmental Science 15, no. 9 (2022): 3583-3602

[14] Pandey, Anand Kumar, and Sheeraz Kirmani. "Multi-objective optimal location and sizing of hybrid photovoltaic systems in distribution systems using a crow search algorithm." International Journal of Renewable Energy Research (IJRER) 9.4 (2019): 1681-1693.

[15] Pandey, Anand Kumar, K. S. Sujatha, and Sheeraz Kirmani. "Minimization of Power Losses with Different Types of DGs Using CSA." International Journal of Renewable Energy Research (IJRER), 10.4 (2020): 1988-1999.

[16] Pandey, Anand K., and Sheeraz Kirmani. "Efficient Approach for DG Placement and Size in Medium Voltage Distribution Systems." 2018 2nd IEEE International Conference on Power Electronics, Intelligent Control and Energy Systems (ICPEICES). IEEE, 2018.